

Wetter
Frejlich

RIAO/OPTILAS 2007

992

AIP

ISBN 978-0-7354-0511-0
ISSN 0094-243X

RIAO/OPTILAS 2007

6th Ibero-American Conference on Optics (RIAO)
and the
9th Latin-American Meeting on Optics, Lasers and
Applications (OPTILAS)

Campinas, São Paulo, Brazil 21 – 26 October 2007

EDITORS

Niklaus Ursus Wetter
Jaime Frejlich

AMERICAN
INSTITUTE
OF PHYSICS

AIP CONFERENCE PROCEEDINGS ■ 992

RIAO/OPTILAS 2007

To learn more about AIP Conference Proceedings, including the
Conference Proceedings Series, please visit the webpage
<http://proceedings.aip.org/proceedings>

RIAO/OPTILAS 2007

6th Ibero-American Conference on Optics (RIAO)

and the

9th Latin-American Meeting on Optics, Lasers and
Applications (OPTILAS)

Campinas, São Paulo, Brazil 21 – 26 October 2007



EDITORS

Niklaus Ursus Wetter

*Institute for Nuclear and Energetic Research
São Paulo, Brazil*

Jaime Frejlich

*IFGW-UNICAMP
Campinas, Brazil*

All papers have been peer-reviewed

SPONSORING ORGANIZATIONS

The State of São Paulo Research Foundation - FAPESP

The State University of Campinas - UNICAMP

The Physics Institute Gleb Wataghin - IFGW

The Brazilian Society of Physics - SBF

The National Council for Scientific and Technological Development - CNPq

The Optical Society of America - OSA

The International Society for Optical Engineering - SPIE

The International Commission for Optics - ICO

The Abdus Salam International Centre for Theoretical Physics - ICTP

The European Optical Society - EOS

The University of Campinas Research Foundation - FAEPEX

The National Council for High Level Education - CAPES

**AMERICAN
INSTITUTE
OF PHYSICS**

Melville, New York, 2008

AIP CONFERENCE PROCEEDINGS ■ VOLUME 992

Editors:

Niklaus Ursus Wetter
Institute for Nuclear and Energetic Research
R. Lineu Prestes 2242
Cid. Universit.
05508-000 São Paulo - SP
Brazil

E-mail: nuwetter@ipen.br

Jaime Frejlich
Laboratório de Óptica
IFGW-UNICAMP
Caixa Postal 6165
13083-970 Campinas - SP
Brazil

E-mail: frejlich@ifi.unicamp.br

The article on pp. 507-512 was authored by a U. S. Government employee and is not covered by the below mentioned copyright.

Authorization to photocopy items for internal or personal use, beyond the free copying permitted under the 1978 U.S. Copyright Law (see statement below), is granted by the American Institute of Physics for users registered with the Copyright Clearance Center (CCC) Transactional Reporting Service, provided that the base fee of \$23.00 per copy is paid directly to CCC, 222 Rosewood Drive, Danvers, MA 01923. For those organizations that have been granted a photocopy license by CCC, a separate system of payment has been arranged. The fee code for users of the Transactional Reporting Service is: 978-0-7354-0511-0/08/\$23.00.

© 2008 American Institute of Physics

Individual readers of this volume and nonprofit libraries, acting for them, are permitted to make fair use of the material in it, such as copying an article for use in teaching or research. Permission is granted to quote from this volume in scientific work with the customary acknowledgment of the source. To reprint a figure, table, or other excerpt requires the consent of one of the original authors and notification to AIP. Republication or systematic or multiple reproduction of any material in this volume is permitted only under license from AIP. Address inquiries to Office of Rights and Permissions, Suite 1NO1, 2 Huntington Quadrangle, Melville, NY 11747-4502; phone: 516-576-2268; fax: 516-576-2450; e-mail: rights@aip.org.

L.C. Catalog Card No. 2008922554
ISBN 978-0-7354-0511-0
ISSN 0094-243X

Printed in the United States of America

CONTENTS

Preface	xvii
Committees	xix

ATMOSPHERIC OPTICS

Aerosol and Water Vapor Raman Lidar System at CEILAP, Buenos Aires, Argentina. Case Study: November 07, 2006.	3
L. A. Otero, P. R. Ristori, and E. J. Quel	
Stratospheric NO₂ Concentration Determined by DOAS Using Compact Spectrographs	9
M. M. Raponi, E. Wolfram, H. Rinaldi, A. Rosales, E. J. Quel, and J. O. Tocho	
Ten Years of Research on Light Propagation through a Turbulent Atmosphere	15
L. Zunino, D. G. Pérez, and M. Garavaglia	
Differential Optical Absorption Spectroscopy (DOAS) Using Targets: SO₂ and NO₂ Measurements in Montevideo City	21
I. Louban, G. Píriz, U. Platt, and E. Frins	
Monitoring Atmospheric Turbulence Evolution by Thin Laser Beams	27
A. Consortini, S. Ceccarelli, and C. Innocenti	

COLOR, VISION AND RADIOMETRY

New Approach for Fast and Accurate Color-Pattern Recognition	33
A. A. Kamshilin, L. Fauch, and E. Nippolainen	
Color Image Sharpening and Application to Eye Fundus Image Analysis	39
E. Valencia and M. S. Millán	
Assessment of the Color Space for the Measure of the Dominant Colors	45
M. Corbalán, E. Valencia, and A. Vega	
Electromagnetic Radiometry and Spatial Coherence Wavelets	51
R. Castaneda and R. Betancur	
Radiometric Analysis of Diffraction	57
R. Castañeda, R. Betancur, J. Herrera, and J. Carrasquilla	
Contrast Sensitivity Test and Conventional and High Frequency Audiometry: Information Beyond that Required to Prescribe Lenses and Headsets	63
S. A. Comastri, G. Martín, J. M. Simon, C. Angarano, S. Dominguez, F. Luzzi, M. Lanusse, M. V. Ranieri, and C. M. Boccio	
Wavefront Aberrations: Analytical Method to Convert Zernike Coefficients from a Pupil to a Scaled Arbitrarily Decentered One	69
S. A. Comastri, L. I. Perez, G. D. Pérez, K. Bastida, and G. Martín	
Study of Light Scattering in the Human Eye	75
I. K. Perez, N. C. Bruce, and L. R. Berriel Valdos	
Automatic Analysis for the Chemical Testing of Urine Examination Using Digital Image Processing Techniques	81
J. M. Vilarly, J. C. Peña, M. F. Daza, C. O. Torres, and L. Mattos	
Hue Discrimination in Iberoamerican Observers	86
J. Carranza and J. Medina	
New Treatment Applying Low Level Laser Therapy for Acute Dehiscence Saphenectomy in Post Myocardial Revascularization	92
N. C. Pinto, N. Shoji, M. Favoretto, Jr., M. Muramatso, M. C. Chavantes, and N. A. G. Stolf	
Improved Pseudo-Colored Engraving Print Method	98
D. Hölck and J. Barbé	
Cover Factor Determination by Means of Reflectance Measurement in Translucent Textile Webs	104
M. Tápías, J. Escofet, and M. Ralló	
Model of the Human Eye Based on ABCD Matrix	108
G. Díaz González and M. D. Iturbe Castillo	

Towards a Brazilian Intercomparison of Radiant Power	114
A. F. G. Ferreira, Jr., J. C. Teixeira, and A. Tada	
Characterization of FEL Lamps as Secondary Standard of Luminous Intensity	120
A. F. G. Ferreira, Jr. and I. E. C. Machado	

DIFFRACTIVE OPTICS

Diffraction Spread of Spatially Partially Optical Fields along the Propagation Axis	129
R. Castaneda, R. Betancur, and J. Carrasquilla	
Diffraction Optical Elements Based in Diamond Like Carbon (DLC) Films	135
M. Sparvoli M. and R. D. Mansano	
Compensation of Inherent Wavefront Distortion in Zero-Twist LCoS Spatial Light Modulators	140
J. Otón, M. S. Millán, E. Pérez-Cabré, and P. Ambs	
Application of LCoS to Dynamical Focusing in an Optical System	146
M. Goldin, G. Díaz Costanzo, O. E. Martínez, C. Iemmi, and S. Ledesma	
Light Intensity Profile Control along the Optical Axis with Complex Pupils Implemented onto a Phase-Only SLM	152
O. López-Coronado, C. Iemmi, J. Davis, J. Campos, and M. J. Yzuel	
The Ronchi Fractional Test	158
C. O. Torres, L. Mattos, G. Baldwin, and Y. Torres	
Waist-to-Waist Transformation of Gaussian Beams Using the Fractional Fourier Transform	163
C. O. Torres, L. Mattos, C. Jiménez, J. Castillo, and Y. Torres	
Fractional Shifting and Sampling in the Fractional Domain. Application to Digital Holography	168
R. Torres, P. Pellat-Finet, and Y. Torres	
Optimization Algorithm for Designing Diffractive Optical Elements	174
V. A. Agudelo and R. Amézquita Orozco	
Constructing White Light Holographic Screens Maximizing Its Size	180
J. J. Lunazzi, D. S. F. Magalhães, and M. C. I. Amon	

EDUCATION FOR OPTICS

Simple Assembling of Organic Light Emitting Diodes for Teaching Purposes in Undergraduate Labs	187
S. Vázquez-Córdova, G. Ramos-Ortiz, J. L. Maldonado, M. A. Meneses-Nava, and O. Barbosa-García	
Using a Photo-Resistor to Verify Irradiance Inverse Square and Malus' Laws	193
A. Dias Tavares, Jr., L. P. Sosman, R. J. M. da Fonseca, L. A. C. P. da Mota, and M. Muramatsu	
Polarization Phase-Shift Interferometry: A Simple Laboratory Setup	199
M. Vannoni, M. Trivi, and G. Molesini	
Research Based Proposal to Learn Optics Better	205
M. C. Menikheim, G. Skop, A. Castellano, and L. I. Perez	
Didactical Holographic Exhibit Including HoloTV (Holographic Television)	210
J. J. Lunazzi, D. S. F. Magalhães, and N. I. R. Rivera	
Web-Based Photonics Training for a New, Flat World	216
D. Sporea, N. Massa, J. Donnelly, and F. Hanes	

GUIDED OPTICS

Contraction Measurements of Dental Composite Material during Photopolymerization by a Fiber Optic Interferometric Method	225
G. Arenas, S. Noriega, V. Mucci, C. Vallo, and R. Duchowicz	
Waveguide Formation by Laser Backwriting Ablation of Metals unto Glass Substrates	231
R. Rangel-Rojo, A. Castelo, M. T. Flores-Arias, C. Gómez-Reino, C. López-Gascón, and G. F. de la Fuente	
Loss Mechanisms and Fluorescence in Photonic Crystal Fibers Filled with Liquids and Polymers	237
J. S. K. Ong and C. J. Santiago de Matos	

Kinetic of Long Period Gratings UV-Induced and Sensing Characteristics	242
R. Z. V. Costa, R. C. Kamikawachi, M. Muller, and J. L. Fabris	
Investigation on the Spectral Properties of Locally Pressed Fiber Bragg Grating Written in Polarization Maintaining Fibers	248
J. F. Botero-Cadavid, J. D. Causado-Buelvas, and P. Torres	
Micro-Engineered Integrated Electro-Optic Modulators in LiNbO₃	254
D. Janner, D. Tulli, M. Belmonte, and V. Pruneri	
Magnetomechanically Induced Long Period Fiber Gratings	260
J. D. Causado-Buelvas, N. D. Gomez-Cardona, and P. Torres	
Application of Artificial Neural Networks for Conformity Analysis of Fuel Performed with an Optical Fiber Sensor	265
G. R. C. Possetti, F. K. Coradin, L. C. Côcco, C. I. Yamamoto, L. V. Ramos de Arruda, R. Falate, M. Muller, and J. L. Fabris	
Intermixing of InP-Based Multiple Quantum Wells for Photonic Integrated Circuits	271
D. A. May-Arrijoja, N. Bickel, P. LiKamWa, and J. J. Sanchez-Mondragon	
Electrically Tunable 2x2 Multimode Interference Coupler	276
D. A. May-Arrijoja, P. LiKamWa, J. J. Sanchez-Mondragon, and M. Torres-Cisneros	

HOLOGRAPHY AND INTERFEROMETRY

Lensometry by Two-Laser Holography with Photorefractive Bi₁₂TiO₂₀	285
E. A. Barbosa and A. O. Preto	
Compact Setup for Reflection Holography with Bi₁₂TiO₂₀ Crystals	291
E. A. Barbosa, A. O. Preto, D. M. Silva, J. F. Carvalho, and N. I. Morimoto	
Multiplexed Transmission Gratings in Dichromated Gelatin Slavich PFG-04 Plates	297
A. Villamarín, J. Atencia, M. V. Collados, and M. Quintanilla	
Analysis of PIV Photographs Using Holographic Lenses in an Anamorphic White Light Fourier Processor Configuration	303
M. V. Collados, J. Atencia, A. M. Villamarín, M. P. Arroyo, and M. Quintanilla	
Application of Biospeckle Phenomenon on Monitoring of Leavening Process in Breadmaking	309
E. R. da Silva, E. da Silva, Jr., M. Favoretto, Jr., S. C. da Silva Lannes, and M. Muramatsu	
A New Estimator for Activity on Dynamic Speckles Based on Contrast of Successive Correlations	314
E. R. da Silva, H. J. Rabal, M. Favoretto, Jr., and M. Muramatsu	
Comparative Study of Analysis Methods in Biospeckle Phenomenon	320
E. R. da Silva and M. Muramatsu	
Human Skull Analysis by Photorefractive Holographic Interferometry	326
G. Caroená, M. Mori, M. R. R. Gesualdi, S. C. Boldrini, E. Ferrara, and M. Muramatsu	
Photorefractive Phase Coupling Measurement Using Self-Stabilized Recording Technique	332
R. Montenegro, I. de Oliveira, A. A. Freschi, and J. Frejlich	
Photoresist Absorption Effect in Holographic Recording	336
L. F. Avila, L. E. Gutierrez-Rivera, J. W. Menezes, W. R. Araújo, and L. Cescato	
Fabrication of Stampers for Molding Polymeric Sieves Using Optical and Holographic Lithography	340
L. E. Gutierrez-Rivera and L. Cescato	
Light Intensity Effects in Photorefractive α-Phase PE-LiNbO₃ Waveguides	344
J. Villarroel, M. Carrascosa, J. Carnicero, A. García-Cabañes, and J. M. Cabrera	
Lippmann Holographic Storage with Homodyne Detection and Single Side Access	350
G. Pauliat, G. Maire, C. Arnaud, F. Guattari, K. Contreras, G. Roosen, S. Jradi, and C. Carré	
Analysis of the Kinetics of Phase and Amplitude Gratings Recorded in Azopolymer Films	356
A. A. Freschi, A. D. S. Cortes, D. A. Donatti, and J. Frejlich	
Semispherical Armonics	361
J. J. Sánchez-Mondragón, A. Dávila-Álvarez, C. A. González-Valdez, A. Alejo-Molina, M. A. Basurto, D. A. May-Arrijoja, J. J. Escobedo-Alatorre, and M. Torres-Cisneros	
Phase Recovery from a Single Interferogram by Region Growing	365
J. Muñoz Maciel, F. J. Casillas Rodríguez, M. M. González, F. G. Peña Lecona, and G. Gómez Rosas	

Propagation of Optical Pulses in Polarization Maintaining Highly Birefringent Fibers	371
A. Leiva and R. Olivares	
Impairments in Gain-Equalized Distributed Fiber Raman Amplifiers due to Four-Wave Mixing and Parametric Amplification Processes	377
M. A. Soto and R. Olivares	
Continuous and Pulsed THz Generation with Molecular Gas Lasers and Photoconductive Antennas Gated by Femtosecond Pulses	383
F. C. Cruz, G. T. Nogueira, L. F. L. Costa, P. F. Jarschel, N. C. Frateschi, R. C. Viscovini, B. R. B. Vieira, V. M. B. Guevara, and D. Pereira	
Energy-Transfer Processes in High Power Yb:Tm:YLF Lasers Emitting at 2.3 μm	386
P. S. F. de Matos, N. U. Wetter, L. Gomes, M. I. Ranieri, and S. L. Baldochi	
Design of a Dual Wavelength Birefringent Filter	392
C. G. Treviño-Palacios, C. Wetzel, and O. J. Zapata-Nava	
Development of a TW Level Cr:LiSAF Multipass Amplifier	398
R. E. Samad, G. E. Calvo Nogueira, S. Licia Baldochi, and N. Dias Vieira, Jr.	
Generation of Photon Pairs with Tailored Spectral Properties by Spontaneous Four-Wave Mixing	403
K. Garay-Palmett, R. Rangel-Rojo, A. B. U'Ren, S. Camacho-López, and R. Evans	
All-Solid State, Single-Frequency Tunable Nd:YLiF₄/ppKTP Red Laser Source for Silver and Calcium Atom Spectroscopy	409
J.-J. Zondy, R. Sarrouf, T. Badr, V. Sousa, and G. Xu	
Pulse-Energy-Enhanced, Strongly Modulated Er:YLF Laser for Medical Applications	415
A. M. Deana, N. U. Wetter, S. L. Baldochi, and I. M. Ranieri	
High Power, Good Beam Quality Nd:YVO₄ Laser Using a Resonator with High Extinction Ratio for Higher-Order Mode Thresholds	420
F. A. Camargo and N. U. Wetter	
Compact Diode-Side-Pumped Nd:YLF Laser with High Beam Quality	426
E. Colombo Sousa, I. M. Raniere, S. L. Baldochi, and N. U. Wetter	
Deep Optical Trap for Cold Calcium Atoms	431
M. Sereno, L. S. Cruz, and F. C. Cruz	
Experimental Study of a Multicavity Fiber Laser System	435
L. C. Gómez-Pavón, J. G. Ortega Mendoza, C. Berrospe-Rodríguez, E. Martí-Panameño, and A. Luis-Ramos	
Describing the Laser Effect in a Substance Modeled by System Constituted by Microsystems of Three Levels of Energy with Variable Optical Pumping Using Package Simulink®	439
R. P. Monsalve, X. Díaz, O. L. Neira B., and A. H. Díaz-Pérez	
Design and Construction of a High Voltage Pulsed Source for Electric Excitation of the Gas Laser	445
X. Díaz, O. L. Neira B., and A. H. Díaz-Pérez	
Optical Frequency Combs Based on Homemade High-Repetition Rate Femtosecond Ti:Sapphire Lasers	451
G. T. Nogueira and F. C. Cruz	
Cluster-Type Entangled Coherent States Generation	454
F. C. Lourenço and A. Vidiella-Barranco	
Partial Polarization and Coherence in Arbitrary Electromagnetic Fields	460
A. T. Friberg	
Influence of Thermal Lensing on the Design of 3 and 4 Mirror Resonators of Ti:Sapphire Lasers	466
V. J. Pinto Robledo and E. Mejía Beltrán	
Generation of States Maximally Entanglement (EPR States) by Passing Two Atoms through Two Coupled Cavities	472
B. F. C. Yabu-uti, F. K. Nohama, and J. A. Roversi	
Measuring Spatial Coherence with a Two-Dimensional Aperture Array	478
A. I. González and Y. Mejía	
All Fiber Laser Using a Ring Cavity	484
A. Varguez Flores, G. Beltrán Pérez, S. Muñoz Aguirre, and J. Castillo Mixcóatl	
DCOOD Optically Pumped by a ¹³CO₂ Laser: New Terahertz Laser Lines	489
R. C. Viscovini, L. F. L. Costa, J. C. S. Moraes, F. C. Cruz, and D. Pereira	

METAMATERIALS

2D Photonic Crystal Layers in Antimony-Based Films	495
J. W. Menezes, M. Nalin, V. F. Rodriguez-Esquerre, H. Hernandez-Figueroa, E. S. Braga, and L. Cescato	
Transfer Matrix and Reflexion in a Metallo-Dielectric Photonic Crystal	501
A. Alejo-Molina, J. J. Sánchez-Mondragón, C. Velásquez-Ordoñez, A. Zamudio-Lara, J. J. Escobedo-Alatorre, D. A. May-Arrijoja, and M. Torres-Cisneros	
Atomic Layer Deposition of Tungsten Thin Films on Opals in the Visible Region	507
Z. A. Sechrist, R. Piestun, and S. M. George	

NONLINEAR OPTICS

Ultra Fast Third Order Nonlinear Response of a Triazole Derivative by Optical Kerr Effect	515
L. Tamayo-Rivera and R. Rangel-Rojo	
Visible to Near-Infrared Continuum Generation in a Watercore Photonic Crystal Fiber	520
A. Bozolan, C. M. B. Cordeiro, C. J. S. de Matos, E. M. dos Santos, and C. H. Brito Cruz	
Automated Z-Scan to Distinguish Different Types of Nonlinearity without Proposing It	524
E. Reynoso Lara, M. D. Iturbe Castillo, C. G. Treviño Palacios, J. A. Dávila Pintle, L. Vela Reyes, and E. A. Martí Panameño	
Evolution of Bright Periodic Lattices in Negative Nonlinear Medium.	530
E. Alvarado-Méndez, M. Trejo-Durán, J. M. Estudillo-Ayala, J. A. Andrade Lucio, G. Anzueto-Sánchez, E. Vargas-Rodríguez, I. Sukhoivanov, and S. Chávez-Cerda	
Organic-Inorganic Hybrid Glass: Non-Linear Optical Properties	536
R. Domínguez Cruz, A. Mendez-Perez, G. Romero Galván, M. Mendoza-Panduro, M. Trejo-Duran, E. Alvarado-Mendez, J. M. Estudillo-Ayala, R. Rojas-Laguna, A. Martínez-Richa, and V. M. Castano	
Chaos Induction in a Laser Diode.	541
M. Reyes and E. Solarte	
Numerical and Experimental Analysis of Modulation Instability and Self-Frequency Shift, in a Standard Single Mode Fibers Pumped by Pulses in Pico- and Nano-Second	547
S. Mendoza-Vazquez, J. L. Camas-Anzueto, E. A. Kuzin, S. Chávez-Cerda, and C. García Lara	
Optical Characterization of Ag⁰ and TiO₂ Nanoparticles	553
A. Espinosa-Calderón, M. Torres-Cisneros, O. G. Ibarra-Manzano, F. R. Arteaga-Sierra, D. A. May-Arrijoja, J. J. Sánchez-Mondragón, C. Velásquez-Ordoñez, and A. Campero	
Experimental Z-Scan Measurements Using Gaussian-Bessel Beams	559
M. M. Méndez Otero, M. L. Arroyo Carrasco, M. D. Iturbe Castillo, G. C. Martínez Jiménez, and F. Rodríguez García	
Comparison between the Morse Eigenfunctions and Deformed Oscillator Wavefunctions.	565
J. Récamier, M. Gorayeb, W. L. Mochán, and J. L. Paz	
Wavelength Converter Based on Four-Wave Mixing in a Bulk Semiconductor Optical Amplifier Assisted by a Sagnac Interferometer and Polarizer	571
M. C. Acosta Enríquez, H. Soto, and R. G. Maldonado Basilio	

OPTICAL INSTRUMENTS

Correlation of Spatially Filtered Dynamic Speckles in Distance Measurement Application.	577
D. V. Semenov, E. Nippolainen, S. V. Miridonov, and A. A. Kamshilin	
Optical-Integrated NH₃ Sensor Design Using WO₃ Thin Films: Influence of Gas Adsorption and Chromic Effects	583
H. E. Lazcano Hernández, C. Sánchez Pérez, and A. García Valenzuela	
New Differential Absorption Lidar for Stratospheric Ozone Monitoring in Argentina.	589
E. A. Wolfram, J. Salvador, R. D'Elia, A. Pazmiño, S. Godin-Beeckmann, H. Nakane, and E. Quel	
Tolerance Analysis of Misalignment for 2D-MEMS Free-Space Optical Cross-Connect.	594
V. Argueta-Díaz and J. T. Yañez-Montiel	
Photometric Passive Range Sensor	600
V. Argueta-Diaz and A. García-Valenzuela	

Characterization of an Optical Device with an Array of Blue Light Emitting Diodes LEDs for Treatment of Neonatal Jaundice	606
P. Fróes Sebbe, A. G. J. Balbin Villaverde, R. A. Nicolau, A. M. Barbosa, and N. Veissid	
Gas Sensor Design Using a Fabry-Perot Interferometer and a Pyroelectric Detector	611
E. Vargas-Rodríguez, H. N. Rutt, R. Rojas-Laguna, and E. Alavarado-Mendez	
Analysis of the Existent Noise in a Gyrocompass of Dynamic Configuration	617
G. E. Sandoval-Romero and S. Palma-Vargas	
Single Sagnac's Interferometers Instrumentation, Based in the Best Detection Limit	622
S. Palma-Vargas, A. Ramírez-Ibarra, and G. E. Sandoval-Romero	
A New Technique to Measure the Width of Gaussian Beams	628
J. A. Dávila, L. V. Reyes, and E. R. Lara	
Implementing and Characterizing a Video Reflectometry Set-Up	632
M. Cunill-Rodríguez, J. Castro-Ramos, S. Vázquez-Montiel, and J. A. Delgado-Atencio	
Alignment Validation of Segmented Mirrors Using Sub-Structured Ronchi Test	638
D. P. Vidal, F. Granados, and A. Cornejo	
Optimization of Optical Systems Using Genetic Algorithms: A Comparison Among Different Implementations of the Algorithm	642
M. E. López-Medina, S. Vázquez-Montiel, and J. Herrera-Vázquez	
Development of Transmissible Photoplethysmography Prototype Sensor Using Polimeric Fiber Optic	648
L. Z. Vilhegas, M. R. Veiga, R. D. Mansano, and J. C. Santos	
Arrangement of the Optical System for Star Testing Using a Spatial Light Modulator	653
N. Bautista-Elivar and C. Robledo-Sánchez	
Free System of Spherical and Coma Aberrations by Use Aspherical and Diffractive Surfaces	659
O. García-Liévanos and S. Vázquez-Montiel	
Spectroscopic Refractometer Using a Double Prism Scheme for Optical Characterization of Liquid Mixtures	665
C. Sánchez-Pérez, V. Leyva-García, A. García-Valenzuela, and R. Soto-Astorga	
Crop Field Reflectance Measurements	671
C. Weber, D. C. Schinca, J. O. Tocho, and F. Videla	
3D Imaging with a Linear Light Source	677
J. J. Lunazzi and N. I. R. Rivera	
Optical Trapping Dynamics in Interference Field	681
L. A. Viera, I. Lira, L. Soto, and C. Pavez	
Novel Stress Sensor Using a Fiber Bragg Grating and a Long Fiber Period Grating	687
I. Santiago N., J. Castillo M., S. Muñoz A., and G. Beltrán P.	

OPTICAL MATERIALS AND APPLICATIONS

Photo-Electromotive-Force from Vibrating Speckled Pattern of Light on Photorefractive CdTe:V	695
T. O. Santos, J. C. Launay, and J. Frejlich	
Temperature and Impurity Concentration Effects on $Mg_{(1-x)}Co_xGa_2O_4$ Photoluminescence	699
L. P. Sosman, A. Dias Tavares, Jr., R. J. M. da Fonseca, and A. R. R. Papa	
Characterization of Photorefractive Materials Using Holographic and Photoconductivity Techniques	704
J. Frejlich, N. R. Inocente-Junior, R. Montenegro, T. O. dos Santos, J. F. Carvalho, K. D. Ferreira, J. C. Launay, and C. Longeaud	
Colour Centre Bragg Grating Recording in Lithium Fluoride Thin Layers	710
F. Bonfigli, M. A. Vincenti, S. Almaviva, R. M. Montereali, E. Nichelatti, H. J. Kalinowski, and R. N. Nogueira	
Parallel Beams and Fans of Rays in Uniaxial Crystals	714
M. C. Simon, L. I. Perez, and F. E. Veiras	
Optimization of the Characteristics of a Quadrant Photodiode	720
A. V. Marquina, D. Berman-Mendoza, and L. A. González	
Development, Characterization and Optimization of an Ultraviolet Silicon Sensor	725
D. Berman-Mendoza, M. Aceves-Mijares, L. R. Berriel-Valdos, J. Pedraza, and A. Vera-Marquina	

Spectral Characterization of a Ferroelectric Liquid Crystal Modulator and Performance Optimization	731
P. Velásquez, P. García, M. M. Sánchez-Lopez, I. Moreno, and F. Mateos	
Confocal and Atomic Force Microscopies of Color Centers Produced by Ultrashort Laser Irradiation in LiF Crystals	737
L. C. Courrol, O. Martinez, R. E. Samad, L. Gomes, I. M. Ranieri, S. L. Baldochi, A. Zanardi de Freitas, and N. Dias Vieira, Jr.	
Incandescent Microlamps Based on MEMS and PECVD Materials	743
G. Rehder, M. I. Alayo, and M. N. P. Carreño	
Optical Characterization of Europium Tetracycline Complex in the Presence of Low Density Lipoprotein and Its Applications	749
F. R. de Oliveira Silva, A. M. Monteiro, A. M. F. Neto, M. A. Gidlund, L. Gomes, N. Dias Vieira, Jr., and L. C. Courrol	
ARROW Waveguides Fabricated with SiO_xN_y and a-SiC:H Films	755
D. O. Carvalho and M. I. Alayo	
Overcoming of the Diffraction Limit for the Discrete Case in Time Reversed Acoustics	761
J. M. Velázquez-Arcos, C. A. Vargas, L. Fernández-Chapou, and J. Granados-Samaniego	
Experimental Analysis of Light Propagation through Supramolecular Chiral Structures in Azopolymer Films	769
G. Martínez-Ponce, C. Solano, R. J. Rodríguez-González, L. Larios-López, D. Navarro-Rodríguez, and L. Nikolova	
Development of a Hybrid Integrated Optics Device	775
A. Rodríguez, M. V. Hernández, S. Guel, G. Ramírez, L. E. Elizalde, and R. Ledezma	
Electrical and Optical Characterization of Porous Silicon/P-Crystalline Silicon Heterojunction Diodes	780
F. Fonthal, T. Trifonov, A. Rodríguez, C. Goyes, L. F. Marsal, J. Ferré-Borrull, and J. Pallarès	
Polymeric Optical Waveguides Fabricated by Plasma Fluorination Process	786
J. R. Bartola, V. M. Giacon, M. I. Alayo, and M. N. P. Carreño	

OPTICAL METROLOGY

Simple Method for Thickness Measurement in Opaque Samples with a Michelson-Sagnac Interferometer	793
E. N. Morel and J. R. Torga	
Extension of Theoretical Model and Improvement on the Data Acquisition Process and the Use of the Biospeckle Technique	798
F. A. Bova	
Insect Wing Displacement Measurement Using Digital Holography	804
D. D. Aguayo, F. Mendoza Santoyo, M. H. de la Torre Ibarra, and C. I. Caloca Mendez	
Low Level Free Vibration Measurements Using High Speed Digital Holography	810
C. Pérez López, F. Mendoza Santoyo, and M. H. de la Torre Ibarra	
Two Dimensional Integration Methods in Polar Coordinates System to Measure the Surface Topography by Optical Deflectometry	816
A. Moreno, M. Espínola, and J. Campos	
Fourier Transform and Temporal Phase Shifting Methods to Measure Vibration Frequency of a Cantilever without Out-of-Plane Conversion	822
C. Meneses-Fabian, G. Rodriguez-Zurita, R. Pastrana-Sanchez, C. Robledo-Sanchez, R. Rodriguez-Vera, and F. Mendoza-Santoyo	
Three-Dimensional Displacement Measurement by Fringe Projection and Speckle Photography	828
B. Barrientos, M. Cerca, J. García-Márquez, and C. Hernández-Bernal	
Influences of the Windowed Fourier Transform on Reliability-Guided Phase Unwrapping	834
J. Garzón, C. López, D. Duque, and J. Galeano	
Topographic Characterization of Corroded Steel Surface	840
J. Garzón, D. A. Duque, C. H. López, and J. A. Galeano	
Measurement of the Topography, Refractive Index and Thickness in Tissues by Mean of a Chromatic Confocal Method	846
J. Garzón, T. Gharbi, and J. Meneses	

Temporal Phase Unwrapping in Structured Perfilometry	852
J. Garzón, J. Galeano, C. López, and D. Duque	
Error Analysis in a Device to Test Optical Systems by Using Ronchi Test and Phase Shifting	858
B. Cabrera-Pérez, J. Castro-Ramos, G. Gordiano-Alvarado, and S. Vázquez y Montiel	
The Geometrical Optics PSF with Third Order Aberrations	864
R. Díaz-Uribe and M. Campos-García	
Temperature Measurement of the Air Convection Using a Schlieren System	870
C. Alvarez-Herrera, D. Moreno-Hernández, B. Barrientos-García, and J. A. Guerrero-Viramontes	
Two-Dimensional Point Shifting for Improving the Quantitative Testing with Null Screens	876
V. I. Moreno-Oliva, M. Campos-García, and R. Díaz-Uribe	
Development of Equipment for Real Time MTF Measurement of Optical Systems	882
D. Rodrigues Romano, S. A. de Almeida Nobre, and B. F. C. de Albuquerque	
In-Fiber Integrated Micro-Displacement Sensor	888
J. D. Causado-Buelvas, N. D. Gomez-Cardona, and P. Torres	
Analysis of Surfaces and Small Dimensions Mechanical Objects with Projections of Fringes Illuminated with Optical Fibers	893
A. Alarcia, K. Contreras, and M. Lomer	
Corrections to the Centroid Evaluation of Spots for a Structured Light System	899
J. A. Jiménez Hernández and R. Díaz Uribe	
Quantitative Shape Evaluation of Fast Aspherics with Null Screens by Fitting Two Local Second Degree Polynomials to the Surface Normals	904
M. Campos-García and R. Díaz-Uribe	
On-Axis Digital Moire Optoelectronic Telemetry	910
P. F. Meilan, A. P. Laquidara, J. A. Bava, and M. Garavaglia	
Optomechatronic Techniques to Characterize the Topography of a MW Satellite Antenna	916
D. Hölck, A. R. R. Molina, P. E. Fluxá, L. M. Zerbino, J. A. Bava, E. C. Cortizo, and M. Garavaglia	
Nanometrology of Deformations by Temperature in Metallic Materials	919
E. F. Mendoza, C. J. Perucho, and A. Plata G.	
Three-Dimensional Profilometry of Solid Objects in Rotation	924
G. Trujillo-Schiaffino, N. Portillo-Amavisca, D. P. Salas-Peimbert, L. Molina-de la Rosa, S. Almazán-Cuellar, and L. F. Corral-Martínez	
Dispersion Equation for a Uniaxial Crystal by Using a Plano-Convex Lens	929
M. Avendaño-Alejo, D. González-Utrera, and R. Díaz-Uribe	
Angular Magnification for a Confocal Off-Axis Optical System	935
M. Avendaño-Alejo, S. Maca García, and R. Díaz-Uribe	
Depolarization of Light Scattered from Rough Cylindrical Surfaces	941
R. Aparicio, F. Perez Quintián, and M. A. Rebollo	
Surfaces Relief Profilometry of Solid Objects by Sweeping of a Laser Line	947
D. P. Salas-Peimbert, G. Trujillo-Schiaffino, P. G. Mendoza-Villegas, D. Ojeda-González, S. Almazán-Cuellar, and L. F. Corral-Martínez	
Study of the Sludge Sedimentation Dynamics by Means of an Optical System	951
J. O. Uc, G. G. Vallejos, C. P. Caballero, C. Q. Franco, and M. Pérez-Cortés	
Temperature Determination with Radial Basis Functions Means of a Nonlinear Common Path Interferometer	957
E. de la Rosa Miranda, L. R. Berriel Valdos, L. I. Olivos-Pérez, and G. Miramontes de León	
Fringe Pattern Demodulation by Independent Windows Fitting Using Genetic Algorithms	963
L. E. Toledo and F. J. Cuevas	
Gas Sensor Using a Rhodamine-6G Doped TiO₂ Film Deposited on an Optical Fiber to Detect Volatile Organic Compounds	969
S. Muñoz Aguirre, C. Martínez Hipatl, J. Castillo Mixcóatl, G. Beltrán Pérez, and R. Palomino Merino	
Fizeau Receiving Interferometer with 2-D CCD Matrix for Low Coherence Interferometric Fiber Optic Sensors	975
M. C. Tomić and Z. V. Djinović	
Laser and Optical Fiber Metrology in Romania	981
D. Sporea and A. Sporea	
Radiant Flux of Near Field in Temperature Measurements	987
J. G. Suárez-Romero, A. J. Reséndiz Barrón, and J. O. Fariás Arguello	

Error-Phase Compensation Properties of Differential Phase-Shifting Algorithms for Fizeau Fringe Patterns	993
M. Miranda and B. V. Dorrió	
Phase Difference Map Interpretation of Mach Diamond Interferometric Patterns by Fourier Transform Methods	999
F. Rodríguez, B. V. Dorrió, and A. F. Doval	
Uncertainty Analysis Using Monte Carlo Method in the Measurement of Phase by ESPI	1005
M. A. Morales, A. Martínez, J. A. Rayas, and R. R. Cordero	
Displacement Fields U and V by Interferometry of Three Beams	1011
A. Martínez, J. A. Rayas, C. Meneses-Fabián, M. Anguiano-Morales, and F. Mendoza	
Frequency Analysis of the Laser Biospeckle	1017
A. M. Enes, G. F. Rabelo, R. A. Braga, Jr., I. M. Dal Fabbro, and M. Vilela	
Application of Phase Shift Projection Moire Technique in Solid Surfaces Topographic Survey	1022
A. C. L. Lino, I. M. Dal Fabbro, and A. M. Enes	
Fruit Surface Topographic Survey Supported by a Phase Shifting Projection <i>Moiré</i> Technique	1028
A. C. L. Lino, I. M. Dal Fabbro, and C. de Almeida	
Application of Phase Shifting Projection Moire on Solid Regular Figures and Plant Organs Three Dimensional Digital Model Generation	1034
A. C. L. Lino and I. M. Dal Fabbro	
Application of Dynamic Speckle Techniques in Monitoring Biofilms Drying Process	1038
A. M. Enes, R. A. Braga, Jr., I. M. Dal Fabbro, W. A. da Silva, and J. Pereira	

OPTICAL PROCESSING

Objective Assessment of Wrinkled Fabrics by Optical and Digital Image Processing	1045
H. C. Abril, E. Valencia, and M. S. Millán	
Optical ID Tags for Secure Verification of Multispectral Visible and NIR Signatures	1051
E. Pérez-Cabré, M. S. Millán, and B. Javidi	
Correlation Based Rotation-Invariant Corner Detector	1057
J. Mazzaferri and S. Ledesma	
Optically Simulated Universal Quantum Computation	1061
D. Francisco and S. Ledesma	
Fractional Fourier Transform Applied to Digital Images Encryption	1067
J. M. Vilarly, C. O. Torres, and L. Mattos	
Three-Dimensional Reconstruction Optical System Using Shadows Triangulation	1073
L. Barba J., L. Vargas Q., C. Torres M., and L. Mattos V.	
Fingerprint Verification by Correlation Using Wavelet Compression of Preprocessing Digital Images	1078
Y. Morales Daza and C. O. Torres	
Digital Color Encryption Using a Multi-Wavelength Source and a Joint Transform Correlator	1083
D. Amaya, M. Tebaldi, R. Torroba, and N. Bolognini	
Optimized Characterization for a Spatial Light Modulator under Less Restrictive Operating Conditions	1088
C. Dorbesi, E. Rueda, M. Tebaldi, R. Torroba, and N. Bolognini	
Frequency Wavelet Filtering Using a Two-Wave Mixing Arrangement in a BSO Crystal	1094
A. Salazar and H. Lorduy G.	
Opto-Electronic Emulation of a Programmable Digital Circuit	1100
E. E. Rodríguez, H. J. Zúñiga, M. L. Calvo, and E. Tepichín	
Wigner Distribution Function of the Images of Quasi-Point Sources in the Vicinity of the Focal Plane	1106
I. J. Orlando Guerrero, J. F. Aguilar, L. R. Berriel Valdós, and J. E. A. Landgrave	
Engraving Print Classification	1111
D. Hölck and J. Barbé	
Detection of a Cosmetic Defect on Lenses Using Wavelets	1117
S. Almazán-Cuéllar, A. Chacón-Aldama, G. Trujillo-Schiaffino, D. Salas-Peinbert, and F. Corral-Martínez	

Application of Laser Shock Processing System by Underwater Irradiation (1064 nm) in Metal Surface	1123
G. Gomez-Rosas, C. Rubio-González, J. L. Ocaña, C. Molpeceres, J. A. Porro, M. Morales, F. J. Casillas, M. Mora-Gonzalez, and F. G. Peña-Lecona	
On the Analogy between Fresnel Diffraction and Dispersion in Transmission Lines and Some of Its Applications	1129
P. Pellat-Finet, Z. Lizarazo, and R. Torres	
Two-Dimensional Temporal Coherence Coding for Super Resolved Imaging through Single Mode Fiber	1135
D. Sylman, Z. Zalevsky, V. Micó, C. Ferreira, and J. García	
Photothermal Spectroscopic Characterization in Core-Shell Quantum Dots Nanoparticles	1140
V. Pilla, R. A. Cruz, T. Catunda, E. Munin, and M. T. T. Pacheco	
Applications of a Visible-LED-Based Resonant Photoacoustic Device	1146
A. Peuriot, V. Slezak, G. Santiago, and M. González	
Identification of Atherosclerotic Plaques in Carotid Artery by Fluorescence Spectroscopy	1151
R. Rocha, A. B. Villaverde, L. Silveira, Jr., M. S. Costa, L. P. Alves, C. A. Pasqualucci, A. Brugnera, Jr.	
Monte Carlo Simulation of Visible Light Diffuse Reflection in Neonatal Skin	1156
J. A. Delgado Atencio, E. E. Rodríguez, A. Cornejo Rodríguez, and J. F. Rivas-Silva	
Global Monitoring of Atmospheric Trace Gases, Clouds and Aerosols from UV/vis/NIR Satellite Instruments: Currents Status and Near Future Perspectives	1160
T. Wagner, S. Beirle, T. Deutschmann, C. Frankenberg, M. Grzegorski, M. F. Khokhar, S. Köhl, T. Marbach, K. Mies, M. P. de Vries, U. Platt, J. Pukite, and S. Sanghavi	
Micro-Crater Laser Induced Breakdown Spectroscopy—An Analytical Approach in Metals Samples	1166
V. Piscitelli, J. Gonzalez, X. Mao, A. Fernandez, and R. Russo	
Thermo-Optical Properties of Nanofluids	1172
M. A. Ortega, L. Rodriguez, J. Castillo, A. Fernández, and L. Echevarria	
Laser-Induced Breakdown Spectroscopy of Alcohols and Protein Solutions	1177
N. Melikechi, H. Ding, A. Marcano O., and S. Rock	
Absorption Spectra of Nitrobenzene Measured with Incoherent White-Light Excitation	1183
H. Cabrera M., A. Marcano O., and J. Ojeda A.	
Comparison between Mode-Matched and Mode-Mismatched Thermal Lens Methods for Absorption Measurements in Liquids	1189
A. Marcano O., H. Cabrera M., and M. Díaz B.	
High-Sensitivity Thermal Lens Optimized Technique to Measure Low Linear Absorption Coefficients	1195
R. A. Cruz, C. Jacinto, A. Marcano O., and T. Catunda	
Increasing Er³⁺ Up-Conversion Intensities By Co-Doping Telluride Glasses With Yb³⁺	1201
J. Jakutis, C. T. Amancio, L. R. P. Kassab, and N. U. Wetter	
Enhancement on the Hypocrellin B Singlet Oxygen Generation Quantum Yield in the Presence of Rare Earth Ions	1207
D. J. Toffoli, L. Gomes, N. D. Vieira, Jr., and L. C. Courrol	
Analysis of the Composition of Titanium Oxide Coating by Laser Induced Breakdown Spectroscopy	1213
H. Estupiñán, D. Y. Peña, R. Cabanzo, and E. Mejía-Ospino	
Study of Biomimetic and Electrolytic Calcium Phosphate Coating on Titanium Alloy by Laser Induced Breakdown Spectroscopy Depth Profiling	1217
H. Estupiñán, D. Y. Peña, R. Cabanzo, and E. Mejía-Ospino	
Intensity Distribution of Laser Induced Plasma Generated at Different Ambient Gas Pressure	1221
R. Sarmiento, R. Cabanzo, and E. Mejía-Ospino	
Comparative Study of Three Fundamental Organic Compounds of Chain Structure of Three Rings—An Approach Based in the Molecular Descriptors of the DFT (Density Functional Theory)	1226
O. L. Neira B., E. F. Mejía, and B. E. Rincón	
Variations in Optical Properties of Silver Nanoparticles. Application in Surface Enhanced Raman Spectroscopy	1232
R. Sato, R. Redón, A. Vázquez, O. Flores, R. Zanella, and J. Saniger	

ATR-FTIR Spectroscopy and Their Applications in the Ring-Opening Reaction of Spiropyran Polymers	1237
R. Delgado Macuil, M. Rojas López, M. Bibbins Martinez, and V. Camacho Pernas	
Optical Properties of Self-Ensemble Monolayers of Gold Metallic Nanostructures	1242
R. Delgado Macuil, V. López Gayou, M. Rojas López, R. Molina Contreras, J. L. García Servin, and J. F. Sánchez Ramírez	
An Array of Photodiodes for Monitoring Hydrocarbons Combustions Burners	1247
L. Arias P., S. Torres I., D. Sbárbaro H., and O. Farías F.	
FTIR Spectroscopy Applied in Remazol Blue Dye Oxidation by Laccases	1253
J. Juárez-Hernández, M. E. Zavala-Soto, M. Bibbins-Martínez, R. Delgado-Macuil, G. Díaz-Godinez, and M. Rojas-López	
Raman and FTIR Spectroscopy of GaSb and Al_xGa_{1-x}Sb Alloys with Nanometric Thickness Grown at Low Temperatures by Liquid Phase Epitaxy	1258
P. Prieto-Cortés, M. Palafox-Plata, V. L. Gayou, R. Delgado-Macuil, A. G. Rodríguez, B. Salazar-Hernández, and M. Rojas-López	
Spectroscopy Stress Evaluation of Translucid Polymers Using Laser Photoelasticity	1262
M. V. Treviño, A. Flores Gil, J. M. Rodríguez-Lelis, A. Hernández González, D. V. Arvizo, M. May Alarcón, and A. Abundez Pliego	
Plasma Emission Spectra of Opuntia Nopalea Obtained with Microsecond Laser Pulses	1268
L. Ponce, T. Flores, A. Arronte, and A. Flores	
Laser Induced Breakdown Spectroscopy of Prickly Pear's Spines and Glochids: A Qualitative Analysis	1274
T. Flores, L. Ponce, G. Bilmes, A. Arronte, and F. Alvira	

THIN FILMS

Optical Excitation of Charge Carriers from Intra-Bandgap States in Ce-Doped SnO₂ Thin Films	1283
V. D. L. Silva, T. F. Pineiz, E. A. Morais, M. A. L. Pinheiro, L. V. A. Scalvi, M. J. Saeki, and E. A. A. Rubo	
Optical Monitoring of Dip Coating: Non-Newtonian Liquids	1289
A. F. Michels, P. Lovato, and F. Horowitz	
Effect of the Pd-Au Thin Film Deposition Technique on Optical Fiber Hydrogen Sensor Response Time	1294
D. Luna-Moreno, D. Monzón-Hernández, D. Martínez, and C. Juárez Lora	
Thin Films IV-VI Semiconductors Compounds with Applications in Optoelectronic Devices by HWBE Growth Technique	1300
S. T. Renosto, L. S. Ribeiro, J. T. de Lima, and S. Guimarães	
Quantum Model for Continuous Photodetection	1306
S. S. Mizrahi, A. V. Dodonov, and V. V. Dodonov	
Microtopographical Characterization of Microcavities on X-Rays Sensor Array	1312
M. F. M. Costa	
Microtopographic Inspection and Fractal Analysis of Skin Neoplasia	1318
M. F. M. Costa, A. V. Hipolito, G. F. Gutierrez, J. Chanona, and E. R. Gallegos	
Phase Estimation in Temporal Speckle Pattern Interferometry Using the Empirical Mode Decomposition Method	1324
F. A. Marengo Rodríguez, A. Federico, and G. H. Kaufmann	
Beam Propagation in a Thick Lens Using the Quantum Mechanics Formulism	1329
H. Lorduy G., L. Castellanos, and Á. Salazar	
Author Index	1335

PREFACE

These Proceedings contains papers presented at the “6th. Ibero-American Conference on Optics and 9th. Latin-American Meeting on Optics, Lasers and Applications” (acronym: “RIO/OPTILAS’07”) that was held in Campinas, São Paulo State, Brazil, between the 21st. and 26th. of October 2007.

The RIO/OPTILAS conferences are held each three years in Latino-American and Iberian countries and are focused on senior and young researchers as well as students working in all areas of Optics, mainly in these countries, but warmly welcoming participants from all over the world.

The present RIO/OPTILAS’07 follows the one held in Venezuela in 2004 and will precede the next one already appointed to be held in Peru in 2010. The most active countries in the area like Argentine, Brazil, Mexico, Spain, Colombia and Venezuela have registered a large number of participants but other countries in the area like Chile, Cuba, Ecuador, Peru, Portugal and Uruguay have also sent a representative number of participants. About 7% of the registered participants came from Europe, USA and Middle-East. It was very stimulating to realize that about 44% of the accepted registered participants were students. An international committee was in charge of selecting the best student posters and thus ten students were awarded with prizes offered by organizations (SPIE, Wiley & Sons) and individuals.

There were 7 plenary invited talks by high quality researcher from Argentine, Germany, Israel, Italy, Mexico and Ukraine and 12 invited contributions from Brazil, Finland, Italy, Spain, UK and Uruguay.. The Book of Abstracts recorded 471 communications divided into 15 different topics with 160 oral communications in three parallel sessions and 311 posters in two special sessions.

We are particularly grateful to SPIE, OSA and ICTP that have provided us with important financial support mainly devoted to support the participation of students in this conference.

We also acknowledge the financial and organizational support from federal (CNPq, CAPES) and state (FAPESP, UNICAMP) national brazilian organizations and institutions as well as scientific national (SBFísica, CePOF) and international (ICO, EOS) organizations that have enabled the successful development of this conference.

We warmly acknowledge the efficient work of all members of the national and international committees that have participated in the organization of the conference and the reviewing of papers.

We are particularly grateful to all those that have made their best to delight us with their interesting and high quality scientific communications.

We also acknowledge the American Institute of Physics (AIP) for offering to us the opportunity to present these Proceedings containing a selection of the most of interesting papers presented in RIAO/OPTILAS'07.

General Chair
Jaime Frejlich
UNICAMP

International Scientific Committee

- Miguel V. Andres (Spain)
- Cid B. de Araújo (Brazil)
- Guillermo Baldwin (Peru)
- Vanderlei S. Bagnato (Brazil)
- Mercedes Carrascosa (Spain)
- Anna Consortini (Italy)
- Manuel Filipe Costa (Portugal)
- Brian Culshaw (U.K.)
- Luiz Davidovich (Brazil)
- Rufino Diaz U. (Mexico)
- Concepcion Domingo (Spain)
- A.A. Friesem (Israel)
- Erna Frins (Uruguay)
- Angela Ma. Guzman H. (Colombia)
- Alexei A. Kamshilin (Finland)
- Guillermo Kauffman (Argentina)
- Arturo Lezama (Uruguay)
- Fernando Mendoza (Mexico)
- Luis Mosquera (Peru)
- Hector Moya (Mexico)
- Jose Luis Paz (Venezuela)
- Hector Rabal (Argentina)
- Y. Tomita (Japan)
- Yezid Torres M. (Colombia)
- Asticio V. Vargas (Chile)
- Maria J. Yzuel (Spain)

Organizing Committee

- Armando Albertazzi (UFSC)
- Isabel Carvalho (PUC-RJ)
- Tomaz Catunda (USP/S.Carlos)
- Ivan de Oliveira (CESET/UNICAMP)
- Dario Donatti (UNESP/RC-SP)
- Pedro V. dos Santos (UFAL)
- Anderson Gomes (UFPE)
- Luis G. Neto (UFSC- S.Carlos)
- Artur da S. Gouveia-Neto (UFRPE)
- Jandir M. Hickman (UFAL)
- Flavio Horowitz (UFRGS)
- Salomon Mizrahi (UFSCAR-DF)
- Carlos Monken (UFMG)
- Sebastião Padua (UFMG)
- José W. Tabosa (UFPE)

Local Committee

- Luis E. E. de Araujo (UNICAMP)
- Eduardo A. Barbosa (FATEC/SP)
- Fernando L. Braga (SBFísica)
- Lucila Cescato (UNICAMP)
- Cristiano Cordeiro (UNICAMP)
- Flavio C. Cruz (UNICAMP)
- Mikiya Muramatsu (USP/SP)
- José A. Roversi (UNICAMP)
- Antonio Vidiella Barranco (UNICAMP)
- Niklaus U. Wetter (IPEN)
- Maria Luisa Calvo (Spain)

Micro-Crater Laser Induced Breakdown Spectroscopy - an Analytical approach in metals samples.

Vincent Piscitelli^{a,b}, Jhanis Gonzalez^b, Xianglei Mao^b, Alberto Fernandez^a, and Richard Russo^b

a UCV- Laboratorio de Espectroscopia Láser, Caracas, Venezuela

b Lawrence Berkeley National laboratory, Berkeley, US

Abstract. The laser ablation has been increasing its popularity like as technique of chemical analysis. This is due to its great potentiality in the analysis of solid samples. On the way to contributing to the development of the technique, we in this work studied the laser induced breakdown spectroscopy (LIBS) in conditions of micro ablation for future studies of coverings and micro crates analysis. Craters between 2 and 7 micrometers of diameter were made using an Nd-YAG nanosecond laser in their fundamental emission of 1064 nm. In order to create these craters we use an objective lens of long distance work and 0.45 of numerical aperture. The atomic emission versus the energy of the laser and its effect on the size of craters was study. We found that below 3 micrometers although there was evidence of material removal by the formation of a crater, it was no detectable atomic emission for our instruments. In order to try to understand this, curves of size of crater versus plasma temperature using the Boltzmann distribution graphs taking the Copper emission lines in the visible region were made. In addition calibration curves for Copper and aluminum were made in two different matrices; one of it was a Cu/Zn alloy and the other a Zinc Matrix. The atomic lines Cu I (521.78 nm) and Al I (396.15 nm) was used. From the Calibration curve the analytical limit of detection and other analytical parameters were obtained.

Keywords: Laser Ablation, Laser induced Breakdown spectroscopy, Micro- craters.

PACS: 52.50.Jm, 52.38.-r, 42.62.Fi

INTRODUCTION

Laser induced breakdown spectroscopy (LIBS) is an atomic emission spectroscopy technique that has the capability to detect, identify and quantify the chemical composition of many material. LIBS utilize a pulsed laser focused on a spot (typically $>20\mu\text{m}$) to create a plasma on the sample surface. The resulting light emission is collected to produce spectrum containing emission lines from the atomic, ionic, and molecular fragments created by the plasma. By properly manipulation of these spectra, elemental chemical analysis both qualitative and quantitative of a wide range of materials can be accomplished [1-4].

LIBS analysis performance depends greatly on the plasma properties and lifetime. In general, to assure adequate plasma lifetime and strong emission intensity, most LIBS setups involve the use of a high energy pulsed laser ($>30\text{mJ}$, depending on the type of laser and wavelength), and large spot sizes ($>20\mu\text{m}$) [4,5]. However, these experimental conditions restrict the spatial resolution (lateral and depth resolution) necessary to access smaller information domains (nanoanalysis and monolayer analysis).

Attempts are being made to push this technology towards miniaturization of the instrumentation; these efforts are mainly driven by the necessity of portable analytical systems rather than improving spatial resolution. However, as is explain below, spot sizes down to less than $10\mu\text{m}$ are used in these miniature systems.

The miniaturization of LIBS systems to compact systems ideal for field deployment have been possible due to the development of small spectrometers, fiber optics, and microchip lasers capable of delivering peak pulses powers up to megawatts [6,7]. Such systems have been used for chemical interrogation of different materials, obtaining analytical figures of merit (precision, accuracy, limit of detection, etc) comparable with the most commonly used LIBS systems, such as those that use high energy Nd:YAG lasers. However, even though there are many advantages by miniaturizing these systems, they also present some drawbacks. For example, microchip lasers can only be

operating at high repetition rates (>kHz), reason for which is required to rotate or scan the samples while they are being ablated, limiting lateral resolution.

In addition, microchip lasers have short pulse widths, in the range of hundreds of picoseconds and they can only deliver pulse energies between 10-50 μ J. Dependency on the pulse widths have been well documented [2,4,8,9], in these papers have been reported that shorter the pulse width shorter the plasma lifetime. Therefore, signal acquisition closer in time to the ablation pulse is required, for which ungated detectors could be used at the risk of increasing the background signal intensity.

Finally, due to the low energy provide by these microchip lasers tight focusing conditions are required to reach breakdown thresholds. And although the small spot size required, theoretically will improve lateral and depth resolution, in fact can introduce new problems. For example, short working distance and shallow focusing depth to such an extent that small changes in the sample surface will move the sample out of focus.

Driven by the increased need of development techniques for nano and monolayer analysis, in this paper is presented a LIBS system in which the crater size can be change between 7-14 μ m using the 1064nm wavelength of a Nd:YAG laser. Signal detection and quantitative chemical analysis is shown. Also a study of plasma emission as a function of the crater size and laser energy is also presented.

EXPERIMENTAL

The first part of this study consisted on making an experimental setup that allow us to create the smallest possible crater permitted by diffraction limitations. For this purpose, the system build works in the focal plane of the objective lens, instead of the image plane which is commonly used in LIBS systems. Working on the focal plane will permit to create craters down close to the optical diffraction limit. Figure 1 show the experimental setup schematics.

A Q-switched Nd:YAG laser ($\tau=4$ ns), operating at its fundamental wavelength (1064 nm) was used to initiate the ablation. The pulse energy was precisely controlled by beam attenuation. The laser beam was directed to the sample using dichroic mirror. Then it was focused using an objective lens (Edmund Optics EO M PLAN HR OBJECTIVE 10X) with a focal length of 19 mm and numerical aperture (NA) of 0.45 and conditioned by a couple of quartz lens. A XYZ motorized stage (Thorlabs RB13S) was used for positioning the sample. Images of the sample were acquired by a camera (Canon PowerShot G7).

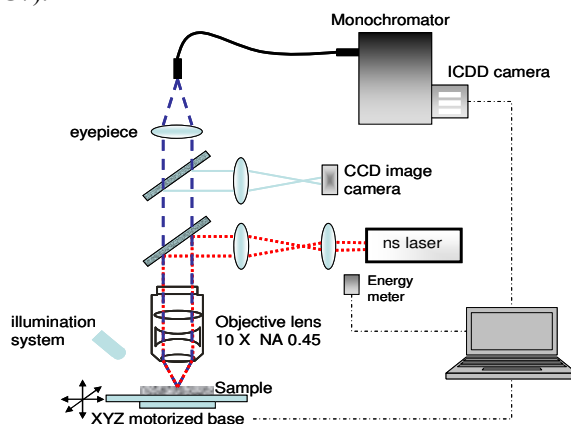


FIGURE 1: EXPERIMENTAL SETUP.

The samples were a series of standard reference materials from the National Institute of Standards and Technology (NIST zinc-base alloys 626-630) and Glen Spectra Inc. (Cu-Zn binary alloys). Table # 1 shows the SRM's compositions. The samples were cutting to an appropriate size and polish even 0.05 μ m alumina powder, cleaned with acetone and storage in a dry cabinet.

The system build for these experiments resembles an optical microscope, even though the focal plane is used instead of the image plane, and the objective lens is used to focusing the laser beam.

The next step was to determine the minimum spot size (energy) from which a reliable signal distinguishable from the background is achievable. For this study the energy was also varied from 1 to 100 μ J and the emission intensity of aluminum ($\lambda=396.15$ nm) and copper ($\lambda=521.8$ nm) were monitored.

TABLE 1. Compositions of the Standard Reference materials.

SRM	Cu	Al	Mg	Fe	Pb	Cd	Sn	Cr	Mn	Ni	Si	~Zn
625	0.034	3.06	0.07	0.036	0.0014	0.0007	6E-04	0.0128	0.031	0.0184	0.017	96.7181
626	0.056	3.56	0.02	0.103	0.0022	0.0016	0.001	0.0395	0.048	0.047	0.042	96.0795
627	0.132	3.88	0.03	0.023	0.0082	0.0051	0.004	0.0038	0.014	0.0029	0.021	95.8758
628	0.611	4.59	0.0094	0.066	0.0045	0.004	0.002	0.0087	0.0091	0.03	0.008	94.6576
629	1.5	5.15	0.094	0.017	0.0135	0.0155	0.012	0.0008	0.0017	0.0075	0.078	93.1100
630	0.976	4.3	0.03	0.023	0.0083	0.0048	0.004	0.0031	0.0106	0.0027	0.022	94.6155

#	Cu	Zn	Zn/Cu
2	55.6	44.4	0.80
4	65.2	34.8	0.53
5	69.5	30.5	0.44
7	82.5	17.5	0.21
9	89.5	10.5	0.12

The last part of this study consisted in building calibration curves using the two series of reference standard materials. Two conditions were set to meet the requirements of this study, improve spatial resolution. These conditions were the use of the smallest spot size from which reliable signal-to-background ratio was obtained (7µm diameter at 41µJ) and one pulse per sample location (10 different locations were ablated to monitor precision). Other optimized parameters used for these experiments were; Gate 300ns, and acquisition delay time 200ns. To collect the emission a 600 µm fiber multimode fiber optics was used. The end part of this fiber was focused into a 15 cm spectrometer with 600 groves/mm gratings and Princeton iCCD as a detector.

RESULT AND DISCUSSION:

Paraxial resolution

The paraxial wave equation that relates laser spot size, numerical aperture and beam quality was used to calculate the minimum spot size permitted by diffraction limits under these experimental conditions. This equation was:

$$S = 2M^2 \frac{\lambda}{\pi NA^{obj}}$$

where S is the spot size diameter, NA^{obj} is the numerical aperture of the objective lens, M² is the beam quality, and λ is the wavelength of the laser radiation. The theoretical spot size for our experimental conditions (NA= 0.45, λ=1064 nm and assuming M²=1), is 1.5 µm and the size of the spot have no dependence with the energy of the laser. However, the crater size could not be experimentally reached since the intensity profile of the spot is strongly dependent on the intensity profile of the radiation, as well as the sample properties. For this reason, the dependency of the crater size with the pulsed laser energy was studied, in order to get the best relation between small crater and detectable emission light for the elements that we was chosen for the studied.

The energy was varied from 1 to 100 µJ. Sample NIST628 was used for this experiment. This sample was chose because the certificated amount of copper is enough to get a strong emission signal and low to avoid the auto-adsorption effects. The importance of the copper lines was based in the fact that whit these emission lines we can calculated the temperature of the plasma using the Boltzmann Plot. In this part of the experiment we fixed the Z sample position to the focal plane of the objective lens, and we vary the laser energy 100 µJ to 1 µJ and collect 20 spectra per energy all of them in different Y sample position. The smallest crater obtained was the 1.7 µm in diameter and 0.5 µm in depth, at laser energy of 1 µJ. this crater is close enough to the theoretical crater predicted using the paraxial wave equation. And as expected, there was a clear correlation (linear) between the pulsed laser energy and the crater size in which, higher the laser energy larger the crater size, figure 2-A. The same tendency was observed for the crater depth, figure 2a insert in figure 2-A shows the crater diameters versus crater depths. It is also important to mention that, in general, if the intensity profile is uniform the spot takes on the Airy disc intensity profile but if the intensity profile is Gaussian, as in this case, the result is an spot of Gaussian profile, as shown in figure 2-B.

Crater size versus emission

The relations between the crater size and the intensity of emission were studied using the sample 628. Figure 4, shows the integrated signals intensities versus laser energy. In this plot it is indicated the energy for which the signal intensity reaches at least three times de background level (3σ). It is also shown the total volume ablated (measured using a white light interferometer microscope (Zygo 200)) at these energies. As is expected, for aluminum (higher concentration) the requirement set for these experiments for the signal level (3σ background) is reached at lower energy than for copper. A minimum energy of $10\mu\text{J}$ (spot size of $5.3\mu\text{m}$) and $27\mu\text{J}$ (spot size of $7\mu\text{m}$) for aluminum and copper, respectively, are necessary to obtain the minimum signal set in this study for chemical analysis.

In order to understand why there was not copper emission measurable when the energy and the crater were less than $27\mu\text{J}$ and $7\mu\text{m}$, respectively. We calculated the excitation temperature from the plasmas form using energies $\geq 40\mu\text{J}$; the Boltzmann plot method was used.

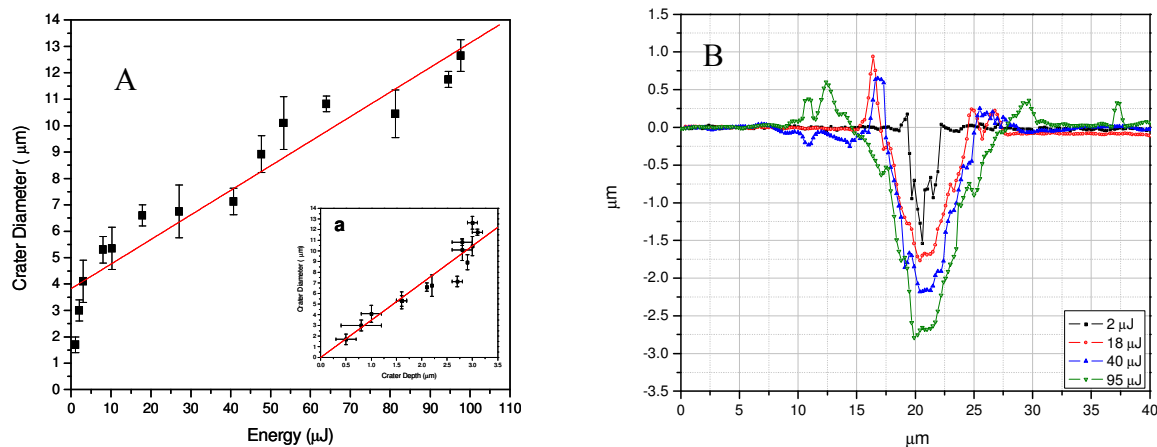


FIGURE 2: 2-A. CRATER SIZE VS LASER ENERGY: NIST 628, 2-B. CRATER PROFILES AT DIFFERENT LASER ENERGIES: NIST 628.

The Cu I emission lines centered at 427.51, 510.55 and 521.8nm were used [10]. The results are showed in figure 5. This figure shows the relation between the plasma excitation temperature and the energy. The plasma excitation temperature decrease when the laser energy decreases. This maybe is due because the amount of material that was removal is lower when the energy of the laser is lower. But also maybe is due that the plasma is so small, that it cold down so fast and no enough thermal energy is available to excite the atoms and promoted its emission. We do have not enough evidence but make sense that a combination of both of this effect is the cause of no emission where the crater size is smaller than $3\mu\text{m}$.

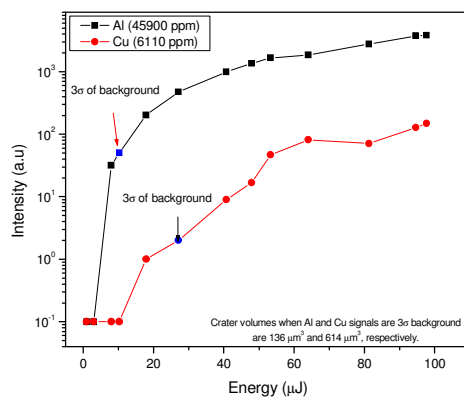


FIGURE 4: SIGNAL INTENSITIES AT DIFFERENT LASER ENERGIES: NIST 628.

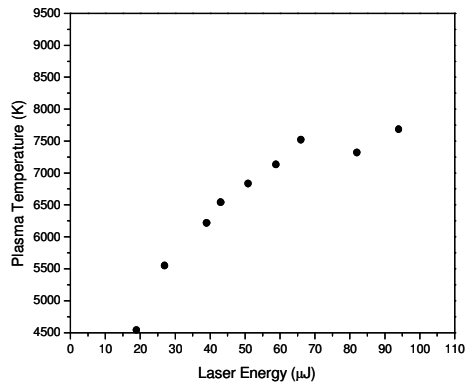


FIGURE 5: PLASMA TEMPERATURE VS. LASER ENERGY: NIST 628.

Calibration Curves

The second part of this work was building the calibration curves for Cu in order to get the analytical merits of the instrument to know which the L.O.D when micro-crater is are used instead the bigger crater.

The calibration curve obtained for NIST 627-630 using these conditions is show in figure 6. The linear regression data in figure 6 gave a correlation coefficient of 0.970 and a limit of detection of 0.1% for Cu. Samples NIST 625 and 626 were not include since they did not meet the requirement of signal-to-background ratio. The calibration curves was made using the area belong the emission peak instead the high of the peak. The 0.1 L.O.D obtained in this work is similar to the L.O.D. obtained by Winefordner et al [6] for similar crater size with the advantage that in this work we can made single crater analysis.

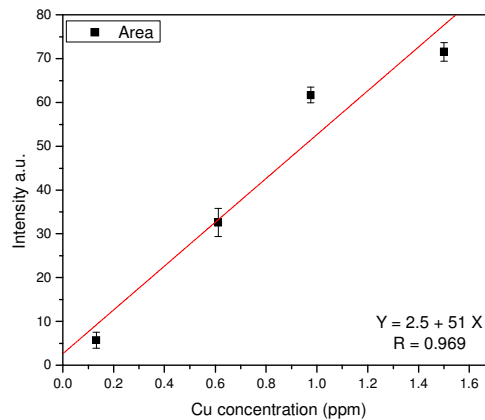
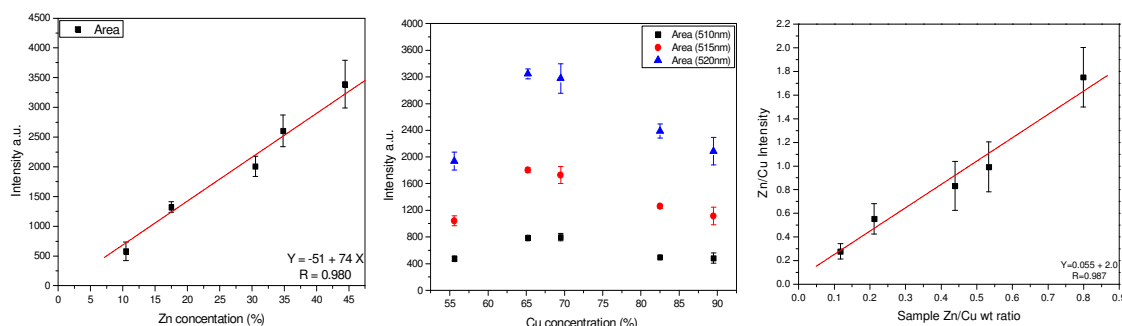


FIGURE 6: CU 520 CALIBRATION CURVE (NIST 625-630 SERIES).

. On the other hand, figure 7, in the same experimental condition the Brass series was study. For those the Cu I (521.8 nm) and the Zn I (481.5 nm) was chose. The first thing that we observed is that for Cu no linear relations was found when we made the graph concentration of Copper versus intensity. Similar effect was observed by Russo et al [11]. The reason of this effect is not well established, but the true is that the seam effect was observed in two different experimental conditions in the same series of sample. In Order to get a better calibration curve for Cu, we made the Zn/Cu ratio in concentration and intensity and the linear square relation obtained was 0.987 and 7 % of LOD for the Copper.



L.O.D.= 7%

FIGURE 7: ZN AND CU CALIBRATION CURVE (BRASS).

CONCLUSIONS

We found in this work, that it is possible to make craters near the limit of diffraction if we used the suitable optics. But these small craters are not able to emit radiation. Possibly to connect this system to a more sensible detector as a mass detector would allow the observation of the elements contained in the target. The smaller crater with emission sufficient to acquire a good spectrum that we could obtain was of 7 μm . the limit of detection as well as the other figures of merits are good enough if we consider the amount of energy provided in this experiment. This type of work opens the door to new experiments on the way to which the microanalysis of samples by means of the laser ablation and in specific of LIBS can be a reality, since they allow knowing the weaknesses and strengths the technique.

ACKNOWLEDGMENTS

CDCH- UCV.
LBNL, Team D, Dr Richard Russo

REFERENCES

- 1 Richard E. Russo, Xianglei Mao, Haichen Liu, Jhanis Gonzalez, Samuel Mao, *Talanta*, **57**, 425-451, 2002.
- 2 E.. Tognoni, V. Palleschi, M. Corsi, G. Cristoforetti, *Spectrochimica Acta Part B*, **57**, 1115-1130, 2002.
- 3 P. Fichet, D Menut, R. Brennetot, E. Vors, A. Rivoallan, *Applied Optics*, **42**, 6029-6034, 2003.
- 4 Jose Vadillo, Javier Laserna, *Spectrochimica Acta Part B*, **59**, 147-161, 2004.
- 5 L. St-Onge, E. Kwong, M. Sabsabi, E.B. Vadas, *Spectrochimica Acta Part B*, **57**, 1131-1140, 2002
- 6 Gornushkin, Amposah-Manager, Smith, Omenetto, Winefordner, *Applied Spectroscopy*, **58**, 762-769, 2004.
- 7 C. Lopez-Moreno, Amposah-Manager, W. Smith, I. GornussKin, N. Omenetto, S. Palanco, J. Laserna, J. Winefordner, *J. Anal. At. Spectroscopy*, **20**, 552-556, 2005.
- 8 P.A. Benedetti, G. Cristoforetti *, S. Legnaioli, V. Palleschi, L. Pardini, A. Salvetti, E. Tognoni, *Spectrochimica Acta Part B*, **60**, 1392 - 1401, 2005
- 9 Zhaoyan Zhang, George Gogos, *Applied Surface Science*,
- 10 K.Meissner, T.Lippert , A.W okaun, D.Guenther, *Thin Solid Film*, 453 -454 (2004) 316-322
- 11 O.V. Borisov , X. Mao, A, Fernandez, M. Caetano, R. Russo. *Spectrochimica acta Part B*, **54**, 1351-1365, 1999